

A flare-associated filament eruption observed in soft X-rays by *Yohkoh* on 1992 May 7

Josef I. Khan^{1*}, Yutaka Uchida², Alan H. McAllister^{3**}, Zadi Mouradian⁴, Irina Soru-Escaut⁴, and Eijiro Hiei⁵

¹ Mullard Space Science Laboratory, University College London, Holmbury Saint Mary, Dorking, Surrey, RH5 6NT, UK

² Department of Physics, Science University of Tokyo, 1-3 Kagurazaka, Shinjuku-ku, Tokyo 162, Japan (uchida@astro1.yy.kagu.sut.ac.jp)

³ High Altitude Observatory, National Center for Atmospheric Research, Box 3000, Boulder, CO 80307, USA (ahm@hao.ucar.edu)

⁴ Department of Solar & Planetary Astronomy, Observatory of Paris, Meudon Section, 5 Place Jules Janssen, F-92195 Meudon Cedex, France (mouradian@obspm.fr)

⁵ Physics Department, Meisei University, 2-1-1 Hodokubo, Hino, Tokyo 191, Japan (hie@solar.mtk.nao.ac.jp)

Received 5 February 1998 / Accepted 19 May 1998

Abstract. *Yohkoh* soft X-ray image data prior to a filament activation and eruption on 1992 May 7 reveal the presence of a bright, filamentary soft X-ray structure apparently lying low under an arcade of soft X-ray loops from which the eruption later originated. This filamentary soft X-ray feature was co-existent and partially co-spatial along the line-of-sight direction with a dark He I 1083 nm filamentary structure (which was similar in appearance to an H α dark filament observed earlier). Prior to the start of the flare the apparently low-lying filamentary soft X-ray structure disappeared, but a bright linear feature was then seen just below several clearly visible overlying loops, consistent with the filamentary soft X-ray feature having risen in altitude. At the same time the H α dark filament became elevated and overlapped well, along the line-of-sight direction, with the elevated linear soft X-ray feature. Some of the overlying loops brightened in soft X-rays at the time the H α data show the H α filament in an elevated position and rising, (but *before* the H α dark filament disappearance). The overlying soft X-ray loops also showed an increase in temperature and emission at the time of the filament activation. Eventually the elevated, filamentary soft X-ray feature disappeared and several apparently cusped shaped loops were then observed in the vicinity. Within several minutes of this time the soft X-ray flare occurred. The series of *Yohkoh* soft X-ray images for this event together with supporting data from ground-based observatories strongly suggest that many features of the magnetic field changes associated with the eruption of the filament were seen in soft X-rays. Moreover the observations indicate that the filament and overlying arcade should be considered to be semi-independent structures that can interact with each other, rather than as parts of a large single structure, as is often assumed. We also find two types of cusped loops in this event. The first type consists of several

distinct narrow cusped loops prior to the flare, while the second type consists of diffuse cusped loop structures which appear to lie above the brightest parts of the bright arcade during gradual phase of the flare. Evidence is also presented which indicates that a nearby parasitic polarity emerging flux region may have played a role in destabilizing the arcade region, causing the filament activation, eruption and flare. The changes in the magnetic field extend beyond the flaring arcade to include the creation of a transient coronal hole and a dark coronal channel near the arcade.

Key words: Sun: corona – Sun: filaments – Sun: flares – Sun: magnetic fields – Sun: X-rays, gamma rays

1. Introduction

Among the interesting phenomena in the solar atmosphere are those where matter with chromospheric characteristics (e.g., temperature, density, etc.) are suspended in the (low) corona. Such features which often take the form of curtain-like or hedge-like structures have long been observed in spectral lines in visible wavelengths used to observe the chromosphere, such as the H α line (656.28 nm). In such lines these features appear in absorption on the solar disk as dark ‘filaments’, while above the solar limb they appear in emission as ‘prominences’ (Tandberg-Hanssen 1995).

Filaments occur both inside and outside active regions and are sometimes observed to ‘disappear’. This disappearance may be due to (i) the heating of the filament material raising it to temperatures outside the range seen by, e.g., spectral lines in visible wavelengths, or (ii) an eruption where (at least a portion of) the filament material may be ejected outward from the Sun. These two cases have been referred to as thermal or dynamical *disparition brusque* (‘sudden disappearances’ in French), respectively (Mouradian et al. 1995). Dynamical *disparition brusque*, i.e., filament eruptions, are usually associated with one particular class of solar flares, the ‘arcade’ (or ‘two ribbon’) flares (Pallavicini

Send offprint requests to: J.I. Khan

* Mailing address: Institute of Space and Astronautical Science, 3-1-1 Yoshinodai, Sagami-hara, Kanagawa 229-0022, Japan (khan@isasxa.solar.isas.ac.jp)

** Now at: Helio Research, 5212 Maryland Ave., La Crescenta, CA 91214, USA

et al. 1977), so-called, because after the filament eruption an arcade of bright loops is seen in soft X-rays (e.g., Sheeley et al. 1975; Webb et al. 1976; Hanaoka et al. 1994; McAllister et al. 1996b). Two or more bright patches are also often seen in $H\alpha$ on either side of the longitudinal component of the (photospheric) magnetic polarity inversion line at the time of the flare (e.g., Smith & Ramsey 1967). Arcade (or two-ribbon) flares are also associated with integrated (spatially unresolved) soft X-ray emission of large peak intensity and long decay times. This type of soft X-ray event is often referred to as a long-duration (or long-decay) event (LDE) (e.g., Sheeley et al. 1975; Kahler 1977). Filament eruptions and LDEs are also associated with coronal mass ejections (e.g., Webb & Hundhausen 1987). While there may be differences between eruptions of quiet region and active region filaments it could be argued that every significant filament eruption is flare-associated. Even when polar crown filaments (or filament channels not obviously loaded with filamentary material) erupt a brightened arcade is formed (e.g., McAllister et al. 1996a) and this may be considered as one aspect of an arcade flare, albeit a weak flare in terms of total soft X-ray flux. Furthermore, Hudson et al. (1994) have shown that even the most thermal-looking (i.e., slowly rising in spatially unresolved soft X-ray emission) long duration events can produce large numbers of accelerated particles, and these may be considered a signature of the primary energy release of a flare.

There have been many reports of the observations of the eruption of filaments. Most of these, however, have been based solely on observations (of material with chromospheric properties) in visible wavelengths, such as the $H\alpha$ line. While such observations may provide some information on the structure and evolution of the magnetic field in the immediate vicinity of the filament, generally speaking, the structure of the coronal magnetic field in the broader vicinity of the filament and on a larger scale, as well as its changes, are not well observed. In particular, while observations of filaments often show that the filament, seen in chromospheric lines, such as $H\alpha$, becomes activated, i.e., rises, before the flare (e.g., Rust 1976), the detailed changes in the soft X-ray features and the coronal magnetic field during such times are not well known. Nonetheless, a number of models for flare-associated filament eruptions have been proposed, along with a variety of topologies for the magnetic structures associated with them (e.g., Priest 1989). Images from the Soft X-ray Telescope (SXT) (Tsuneta et al. 1991) on board the *Yohkoh* satellite (Ogawara et al. 1991) show the structure of the magnetic field in the corona, and from these it is now possible to obtain a better understanding of the topological changes occurring in the coronal magnetic field before, during and after a filament eruption.

In this paper we present an analysis of observations of a flare-associated filament eruption which occurred on 1992 May 7. Preliminary analysis was carried out by Khan et al. (1994). The present paper presents a detailed analysis of the observations of this event, based mostly on *Yohkoh* SXT data with contextual ground-based data. The analysis reveals interesting observational features in the evolutionary development of this fila-

ment activation and eruption, especially in the stages prior to and early in the flare.

In Sect. 2 the basic observational findings from $H\alpha$ data from Paris-Meudon Observatory along with other ground-based data are described. A detailed description of the changes in morphology and brightness of soft X-ray features (and by inference in the magnetic field) as seen with the *Yohkoh* SXT is given in Sect. 3. This is followed by a brief comparison of the soft X-ray features seen with the SXT with the features seen in the $H\alpha$ images in Sect. 4. In Sect. 5, we propose a possible interpretation of this event based on the observations. The main conclusions are summarized in Sect. 6.

2. Ground-based and GOES observations

According to the listing produced by the Solar-Terrestrial Physics Division of the National Geophysical Data Center (NGDC) of the National Oceanic and Atmospheric Administration (NOAA), USA which is based on observations from terrestrial instruments and from the *Geostationary Operational Environmental Satellite (GOES)*, a flare of $H\alpha$ optical importance 2F and X-ray class C3.4 occurred on 1992 May 7 with start, peak, and end times of about 06:23 UT, 07:15 UT, and 07:44 UT respectively. The flare was located at the approximate heliocentric coordinates of S23E48.

There were also reports of Type II and Type IV radio bursts associated with the flare. These types of metric radio bursts are often associated with filament eruptions. Type II bursts are generally believed to be due to plasma emission produced by electrons excited by magnetohydrodynamic shock waves caused by a flare (Uchida 1974; Nelson & Melrose 1985). Kozuka et al. (1995) examined the interplanetary consequences of this event and suggested that a shock, inferred from interplanetary scintillation of radio waves from a quasar, was related to the Type II shock. According to the NGDC listing a bright surge on the limb was also reported in association with this flare.

$H\alpha$ images from various sites around the world indicate that a filament was located near the magnetic polarity inversion line where the eruptive event eventually occurred as the region appeared from behind the east solar limb (i.e., well before the flare). Fig. 1a–f shows relevant portions of $H\alpha$ filtergrams from Paris-Meudon Observatory before, during and after the flare on May 7. Although it is not our intention to discuss in detail the changes seen in $H\alpha$, we briefly describe the main interesting features. The $H\alpha$ development of this event is discussed in Mouradian et al. (1998).

The filament which eventually disappeared is indicated by the arrow with the solid head in Fig. 1a. (All the figures consisting of image data in this paper are portions of full-disk images and show the scale size of thirty SXT half-resolution pixels; 2.5 arc minutes. Moreover, solar north is always up and solar east is to the left. All $H\alpha$ images are positives, while all SXT images are negatives.) In Figs. 1b–d we indicate parts of the filament which can be identified although we do not discuss the detailed changes. Fig. 1e shows the $H\alpha$ two-ribbon flare emission, while Fig. 1f shows faint emission in the former location of the ribbons

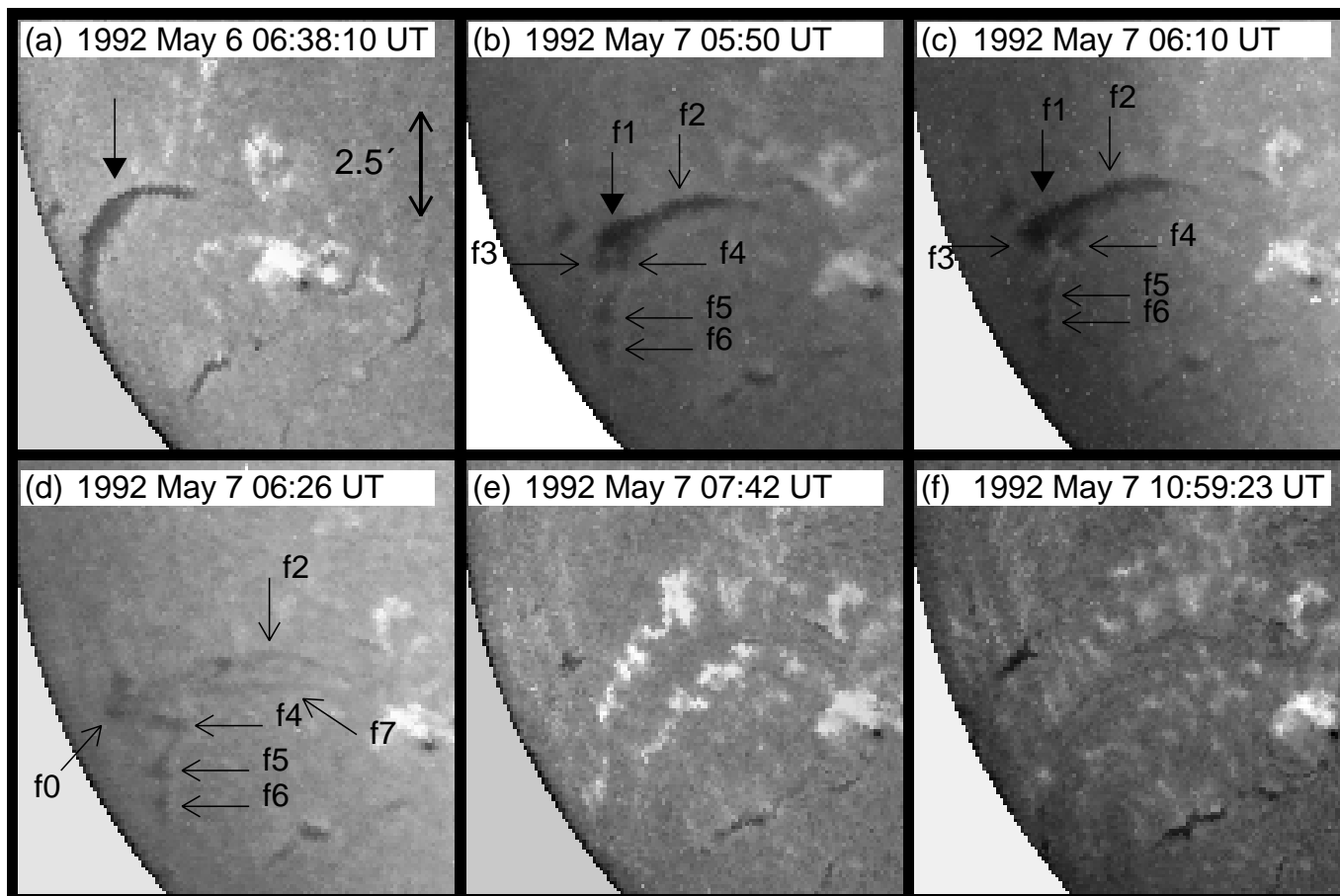


Fig. 1a–f. Portions of full-disk $H\alpha$ filtergrams from Paris-Meudon Observatory. The arrow with the solid head in **a** indicates the $H\alpha$ dark filament which eventually erupted. Parts of the $H\alpha$ dark filament are indicated and labeled in **b–d**. These images show the $H\alpha$ line center intensity and are displayed on a linear scale.

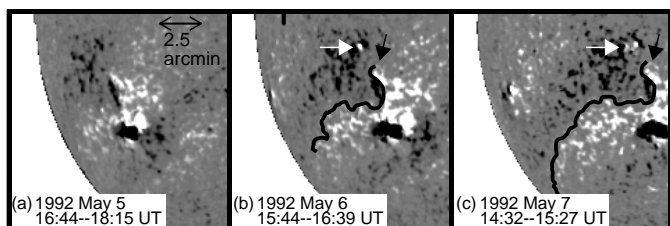


Fig. 2a–c. Portions of full-disk magnetograms from NSO showing the line-of-sight photospheric magnetic field. The magnetic field values are truncated above 10 mT and below -10 mT and are displayed on a linear scale. White is positive (i.e., towards the reader) and black is negative (i.e., away from the reader).

and the beginning of the appearance of an $H\alpha$ dark filament near the magnetic polarity inversion line.

From magnetogram data obtained from the National Solar Observatory (NSO), Kitt Peak, USA, we examined strong and weak values for the line-of-sight photospheric magnetic fields in the region of the flare and filament eruption. Relevant portions of magnetograms showing weak fields taken before and after the flare are shown in Fig. 2a–c. These images show the line-of-sight magnetic field truncated above absolute magnitude

10 mT (100 G). The images are shown in a linear color table and the scaling is consistent such that the relative differences can be compared between the images. The emergence of magnetic flux (indicated by the white arrow) away from the magnetic polarity inversion line (indicated by the thick black line) about a day before the May 7 flare, can be clearly seen in Fig. 2b. Examining the untruncated data, this small emerging flux region had a significant line-of-sight positive polarity magnetic flux component (~ 20 – 35 mT) emerging in a region with mostly negative polarity of $\sim (-20)$ – (-10) mT. Such photospheric magnetic features have generally been referred to as parasitic polarity regions (Martres et al. 1966). In Sect. 3.3, we discuss the role this region may have played in the filament eruption and flare. In contrast, we provide evidence which indicates that the strong bipolar region straddling one end of the (photospheric) magnetic polarity inversion line (indicated by the black arrow in Figs. 2b and 2c) did not appear to have played a significant role in the filament eruption.

Fig. 3 shows the soft X-ray flux from the *GOES 7* low energy channel (~ 0.1 – 0.8 nm) and high energy channel (~ 0.05 – 0.4 nm), with times of *Yohkoh* satellite night shown in the filled areas between dotted vertical lines. From this it can readily

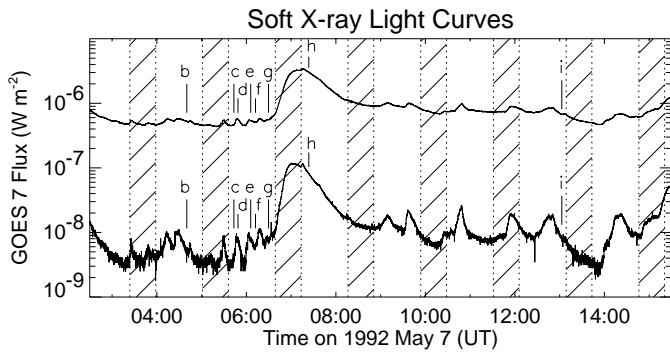


Fig. 3. Time profiles of the ~ 3 second *GOES* 7 integrated soft X-ray flux for the low energy channel (~ 0.1 – 0.8 nm) (the higher intensity) and the high energy channel (~ 0.05 – 0.4 nm) (the lower intensity) for times near the flare on 1992 May 7 discussed in this paper. The tick marks and labels refer to the times of images shown in Fig. 4.

be seen that *Yohkoh* missed the rise of the flare. Nonetheless, *Yohkoh* observed interesting activity before the flare as well as during and after the gradual phase of the flare. Also indicated in Fig. 3 are the times of some of the *Yohkoh* SXT images presented in Fig. 4a–i. Note that from the *GOES* plot shown in Fig. 3 the flare appeared to last ~ 2 hr, perhaps more, above the background level. While the durations of LDEs are not precisely defined (Sheeley et al. 1983), based on the *GOES* light curve this flare appears to be at the low end of durations for LDE flares. However see Sect. 3.2.1 where we briefly discuss the spatially resolved soft X-ray intensity of the flaring arcade.

3. *Yohkoh* soft X-ray observations

To illustrate the development of the soft X-ray features associated with this event several representative images are shown in Fig. 4a–i. These are portions of *Yohkoh* SXT full-disk images taken with the two ‘thinnest’ soft X-ray filters; one consisting of a thin layer of Al, abbreviated as the Al.1 filter and the other a composite filter consisting of Al, Mg, Mn and C, abbreviated as the AlMg filter (Tsuneta et al. 1991). The images were corrected using standard *Yohkoh* software and were aligned to track a position near the center of the soft X-ray arcade which flared (heliocentric coordinates S23E50 at 07:23:42 UT on 1992 May 7) assuming differential rotation. The output values of the pixels of the images were normalized to yield ‘uncompressed SXT digital data numbers’ (described below) per second, such that the relative differences between images could be compared. Each image is scaled logarithmically and the values were stretched linearly to span the full range of display values for each image. Thus the relative differences between the images cannot be compared directly from this figure. Displaying the images in this way shows the most important features at the time of each image and, also exaggerates the apparent brightness of the fainter features thereby showing more of the magnetic structures. The images were expanded in size and smoothed using bilinear interpolation and displayed using a reverse (linear) black and white color table. (These general processing and display procedures have been applied to all the SXT images presented in this pa-

per.) Some of the images show pixel saturation effects (which are apparent as vertical or triangular streaks from NOAA Region 7154 in all panels, except Fig. 4c and Fig. 4h, and as well as from the bright structure to the north of NOAA Region 7154 in Fig. 4d). These features should, of course, be ignored.

Some words are in order about the output of the *Yohkoh* SXT. The SXT is a digital camera consisting of 1024×1024 pixels. The full-disk images of the Sun used here consist of 512×512 or 256×256 pixels. These are obtained by on-board summation of 2×2 and 4×4 pixels, respectively. When a soft X-ray photon strikes a pixel of the SXT it produces electron-hole pairs in the silicon layer of that pixel. From the number of electrons produced in each pixel an output quantity is calculated which is referred to as uncompressed digital data numbers or DN. Since the soft X-ray flux of the Sun is not mono-energetic the output for each SXT pixel is *not* directly related to the actual number of photons striking the CCD. Rather the total number of electrons produced in each pixel is a measure the soft X-ray photon flux integrated over the range of energies to which the SXT pixel is sensitive (~ 0.28 – 4 keV corresponding to ~ 0.3 – 4.5 nm). Photons of different energies produce different numbers of electrons. Assuming a fixed wavelength, it is possible to estimate the number of photons striking an SXT pixel. However since our purpose here is to show the development of soft X-ray features we feel it is appropriate to simply show images of SXT digital data numbers.

In order to aid discussion of the development of the soft X-ray structures in this event it is helpful to describe and label the features in the region which produced the filament eruption and flare. *Yohkoh* SXT observations indicate that the morphology of this region prior to the filament activation and the flare consisted of the following principal structures in soft X-rays: (a) A bright, compact region north of NOAA region 7154, corresponding to an H α plage region which was eventually labeled NOAA region 7157; (b) A relatively bright, densely packed ‘arcade’ of loops (more like a tight cluster or bundle of loops than a uniform arcade) lying immediately adjacent to and partially overlying the aforementioned region; (c) A faint arcade of loops extending south-eastward which may be an extension of the ‘arcade’ described in (b). These structures are referred to as Regions A, B, and C respectively, and are shown labeled in Fig. 4b which is a portion of a full-disk soft X-ray image of the Sun taken with the *Yohkoh* SXT. The pre-existing soft X-ray configurations in these structures seem to have remained fairly unchanged from the time they emerged from behind the east limb of the Sun until at least $\sim 04:42$ UT on May 7. However a new structure did appear early on May 6 corresponding to the emerging flux region discussed above. This is indicated by the arrow in Fig. 4a and is also shown labeled as Region D in Fig. 4b. This was eventually labeled NOAA region 7161.

The evolution of the soft X-ray structures observed with the *Yohkoh* SXT can be divided into the following consecutive stages: (i) a fairly long-lasting pre-existing configuration, (ii) the appearance of Region D, (iii) distortions and brightenings of the loops of Region C prior to the flare, (iv) the start of the flare, (v) the rise and peak of the flare (which was missed by

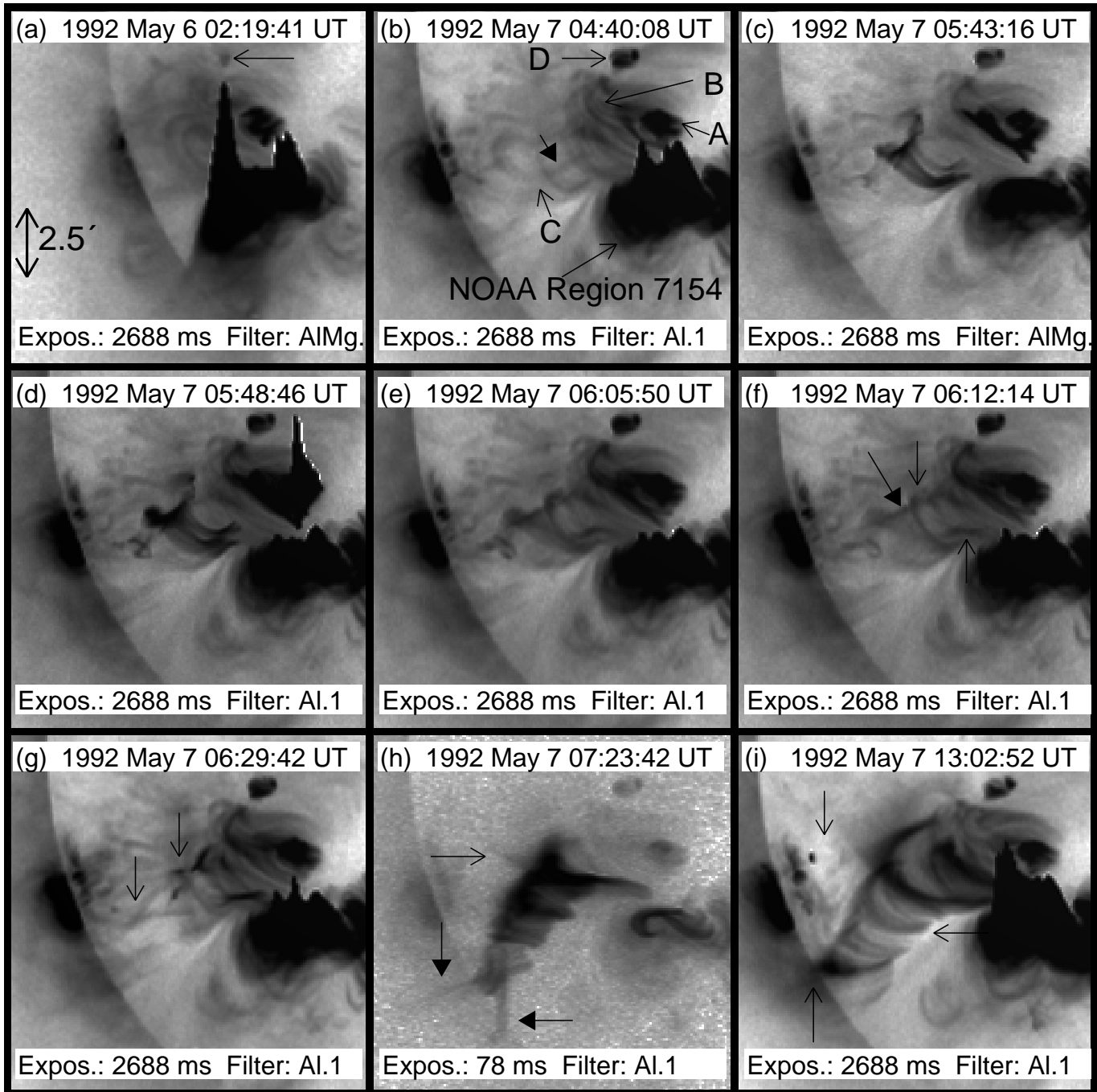


Fig. 4a–i. Portions of full-disk images taken by the *Yohkoh* SXT showing the development of soft X-ray structures relating to the filament eruption and flare on 1992 May 7. The images are of SXT digital data numbers per second (described in the main text). These images are expanded and smoothed using bilinear interpolation and displayed using a reverse color table in which the data values for each image are individually scaled logarithmically and then stretched linearly to span the full range of display values for each image. In **b** the long-lasting pre-flare configuration is shown with labeled regions which are described in the main text. The original soft X-ray filters and exposure durations of the images are shown in each panel. In particular, note that **h** was taken during the flare and is of much shorter duration.

Yohkoh because of satellite ‘night’), (vi) the gradual phase of the flare, and (vii) the post-flare phase. For most of this paper we concentrate on the evolution of Region C which initially appeared to be a faint arcade and was later the site of a dynamic arcade associated with the filament eruption.

3.1. Outline of pre-existing soft X-ray configuration

Fig. 4b shows that several large loops can be seen clearly in Region C long before the flare. Also visible in emission in soft X-rays (indicated by the arrow with the solid head in Fig. 4b is a long, thin structure apparently lying low near the magnetic

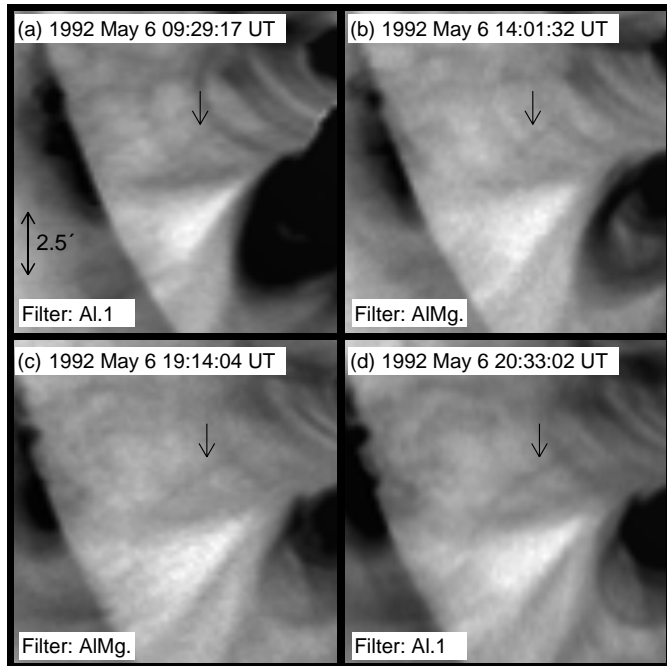


Fig. 5a–d. Portions of full-disk images taken by the *Yohkoh* SXT showing a long, thin filamentary structure in emission in soft X-rays apparently lying low near the magnetic polarity inversion line under an arcade of loops from which a filament eruption and flare occurred on 1992 May 7.

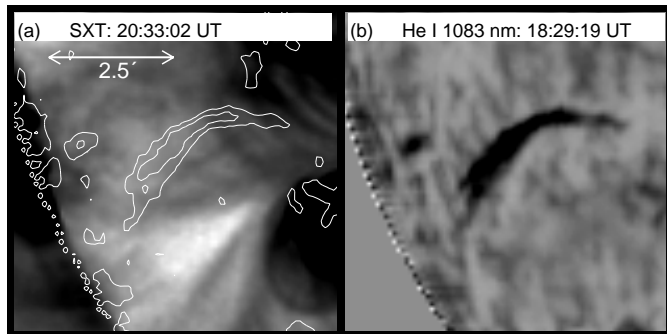


Fig. 6. a A portion of full-disk images taken by the *Yohkoh* SXT showing a filamentary structure in soft X-rays (part of that shown in Fig. 5d), and **b** a He I 1083 nm image from NSO, Kitt Peak, USA, taken on 1992 May 6 artificially rotated forward in time to the time of the image in **a**. Contours of **b** are shown overlaid on **a**.

polarity inversion line, i.e., near the axis of the overlying faint arcade of loops. This filamentary soft X-ray feature was fairly long-lived. Fig. 5a–d shows several images which demonstrate that it was present at least 10 hr and perhaps 20 hr, before the flare on 1992 May 7.

The long thin soft X-ray feature appears roughly similar in size, shape, and inferred line-of-sight position with the $H\alpha$ dark filament described in Sect. 2. It also overlaps in time with a dark filamentary feature seen in images taken in the He I 1083 nm line. The soft X-ray and He I 1083 nm filamentary structures were clearly co-existent since the dark He I 1083 nm line feature was visible until at least $\sim 18:29$ UT on May 6 while the bright

filamentary soft X-ray structure was visible low under the arcade from at least $\sim 14:01$ UT on May 6 and perhaps earlier. Shown in Fig. 6 is the soft X-ray image from Fig. 5d (on a logarithmic scale) overlaid with the contours from an He I 1083 nm image (on a linear scale) from NSO, Kitt Peak, USA, which is rotated slightly (assuming differential rotation) to match the time of the SXT image. The rotation rate used is that observed for small magnetic features taken from Howard et al. (1990). Projection errors for the rotated dark filamentary feature are small due to the small amount of rotation (~ 1 – 3 SXT half resolution pixels) applied to this data. The overlay indicates partial overlap, along the line-of-sight direction, of the dark He I 1083 nm filamentary feature and the thin, bright soft X-ray structure.

Although the interpretation of bright and dark features seen in the He I 1083 nm line can sometimes be complicated, it is reasonable to treat the dark He I 1083 nm filamentary feature as a proxy for the $H\alpha$ dark filament since the $H\alpha$ dark filament and the dark He I 1083 nm filamentary feature appear to be similar in earlier images. To simplify the discussion the thin, bright, apparently low-lying filamentary soft X-ray structure seen in Fig. 4b, Fig. 5a–d and Fig. 6a will be referred to here simply as the ‘bright filament’. To our knowledge, such a feature, seen several hours before the filament activation, has not been reported before in the literature. The coincidence in time and approximate line-of-sight location of the ‘bright filament’ and the dark He I 1083 nm filamentary feature (and by inference the $H\alpha$ dark filament) suggests an association between these structures. The possible temperature of filament material based on observations in, e.g., visible wavelengths, is $\sim 10^3$ – 10^4 K (Tandberg-Hanssen 1995), whereas the possible temperature for bright features seen with the *Yohkoh* SXT start at $\sim 10^6$ K (Tsuneta et al. 1991). We are unable to estimate the temperature of the arcade, Region C, and the ‘bright filament’ accurately, due either to poor statistics or lack of appropriate filter pairs. Nonetheless, using the filter ratio technique for the SXT images (Hara et al. 1992) we find that the features for which we can determine the temperature (Regions B and parts of Regions C, including possibly the ‘bright filament’) all appear to be ~ 2 MK. It is reasonable to suppose that the temperature of the arcade and ‘bright filament’ are similar, ~ 2 MK. The different temperatures of the dark and ‘bright’ filamentary structures shows that they are certainly not the same material at the same time. The exact location of the soft X-ray structure relative to that of the dark filament is not clear. We will discuss this further in Sect. 5 where we discuss the interpretation of the dynamical evolution of various soft X-ray features.

3.2. Dynamic arcade region (Region C)

3.2.1. Soft X-ray development

The *Yohkoh* SXT images show that there was a long-lasting period before the flare where the soft X-ray structures of Regions A, B and C did not show significant change. The last *Yohkoh* SXT image clearly showing these relatively unaltered structures was taken at 04:42:16 UT on May 7. Another image

near this time is shown in Fig. 4b. After these few images there was a gap in the *Yohkoh* data due to satellite ‘night’.

After the data gap, the loop structures in Region C appeared to be notably ‘distorted’ and were much brighter. An image taken at 05:43:16 UT (shown in Fig. 4c) clearly shows bright ‘distorted’ loops in Region C. The details of the configuration early in this stage are not entirely clear. However, in the images taken shortly afterwards, the ‘bright filament’ is no longer visible apparently lying low under the arcade near the magnetic polarity inversion line. Instead, a narrow, ‘rail’-like feature is seen in emission near the top of the much brighter loops (indicated by the arrow with the solid head in Fig. 4f). The overlying loops seem to be wrapped closely around this ‘rail’. At first appearance of the ‘distorted’ loops, they seem to arch over the bright ‘rail’-like structure and appear to be compressed together, giving the impression that they are pulled or pushed together and upwards at their tops.

After some time a clearly distinguishable loop is seen arching over the ‘rail’ feature and is indicated by the southward-pointing arrow in Fig. 4f. There is another flux ‘loop’ which appears to thread through this loop and then possibly twists around the ‘rail’. This is indicated by the northward-pointing arrow in Fig. 4f.

While the rise phase of the (soft X-ray) flare was missed due to *Yohkoh* satellite ‘night’ we were fortunate to obtain one image just prior to the flare which shows interesting features. That image was taken at 06:29:42 UT and is shown in Fig. 4g. Note that in this image the configuration in Region C has changed markedly. The ‘rail’ which was previously near the top of the loops of the arcade has now disappeared. Instead, several ‘loops’ which appear to be ‘cusped’ at their tops are now clearly visible. These apparently ‘cusped’-shaped loops seem to be oriented in different directions. The NOAA event listing gives the center of the flare as heliocentric coordinates S23E25 (presumably, the location of the centroid of the $H\alpha$ flare ribbons). This is centered on the region of the cusped loops. Careful examination of the *GOES* soft X-ray flux shows a gradual increase starting at \sim 06:31 UT. The *GOES* soft X-ray flux continued to rise gradually until \sim 06:38 UT when it showed a steeper rise. The time of the ‘cusped’ loops is the time of the last stage of the magnetic reconfigurations associated with the eruption. Depending on the interpretation of the ‘cusped’ loops, this could be considered to be the time of (i) part of the pre-flare phase or (ii) the start of the primary energy release of the flare (assuming that high energy particles are accelerated at that time).

After the single image which showed the cusped loops and a gap in the data due to satellite ‘night’ the *Yohkoh* SXT captured images of the gradual phase of the flare. A representative image is shown in Fig. 4h. An arcade of brightened loops, formed after the eruption of the $H\alpha$ filament, is visible in Region C. This arcade structure clearly extends south-eastwards.

We also point out the appearance of interesting features at the southeastern end of the arcade at the time of the flare as indicated by the arrows with the solid heads in Fig. 4h. These features may be the end of the dynamic changes in the arcade associated with the flare and the filament eruption. They consist

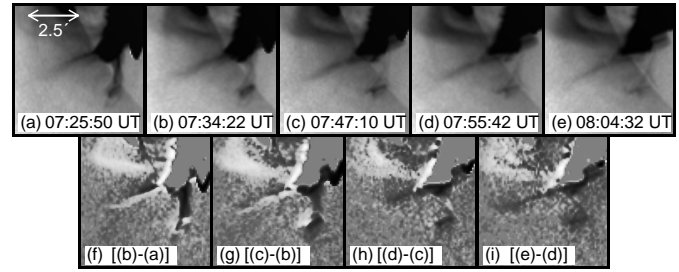


Fig. 7. Panels a–e are a sequence of SXT images showing the features at the end of the flaring arcade, Region C, on 1992 May 7. Panels f–i shows difference images between consecutive images in a–e. Together these sets of images show apparent motion of the soft X-ray emitting plasma of the features at the end of the arcade. White is positive (i.e., denotes increase in emission), while black is negative (i.e., denotes decrease in emission).

of what look like two linear soft X-ray features with a ‘knot’ located near where they meet. Examining these features we find evidence for outward motion most markedly in the feature to the east. There is also an apparent twisting motion of the features, especially the feature to the west. Fig. 7 shows a sequence of images illustrating this apparent motion. The data shown in this figure consist only of images taken with an exposure duration of 2668 ms with the Al.1 soft X-ray filter. The images are scaled separately so the apparent relative differences in intensity between the images (a)–(e) are deceptive. However, Figs. 7f–7i are scaled so that positive differences appear light-colored while negative differences appear dark-colored. The flare examined here was reported as being associated with a bright surge (i.e., a collimated plasma flow) at the limb. The soft X-ray ‘tail’ features extend beyond the limb and show motion, so they may be related to the surge. A surge-like feature corresponding to the soft X-ray feature to the east is visible in $H\alpha$ filtergrams from Paris-Meudon Observatory from \sim 06:54 UT to \sim 08:41 UT on May 7, with a maximum intensity at \sim 07:35 while the soft X-ray features are visible from \sim 07:23 UT to \sim 08:06 UT. The soft X-ray feature to the west appears to lie near the filament section f6 in Fig. 1a–f and may even be part of a surging prominence.

The general appearance of bright soft X-ray structures in Fig. 4h superficially resemble a shrimp and so we refer to this flare as the *ebi* flare (using the Japanese term for ‘shrimp’: Regions A and D being the eyes, Regions B and C the body, and the features at the end of Region C being the tail).

The arcade of loops of Region C gradually decreased in brightness with time. Nonetheless, a bright arcade remained long after the *GOES* soft X-ray flux (Fig. 3) dropped to the background level (Fig. 4i). Momentarily jumping ahead to Fig. 10, we see the temporal variation of the intensity of boxed region u which is part of Region C. The intensity of the spatially resolved soft X-ray flaring arcade actually lasted \sim 10 hr, much longer than the LDE seen in the integrated *GOES* plot (Fig. 3). Thus this flare does have a duration typical of LDEs, but is of relatively low total soft X-ray intensity.

Eventually most of the ‘tail’-like features at the end of Region C disappeared, leaving a diffuse feature over the southern-

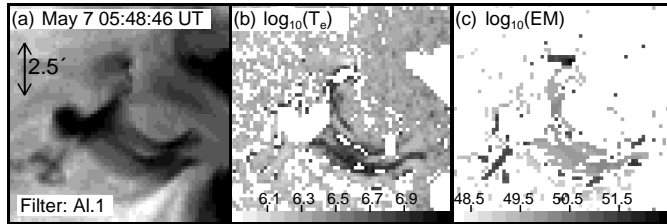


Fig. 8. **a** Shows a portion of the soft X-ray image shown in Fig. 4d. Using this image and an interpolated image obtained from images taken with the AlMg filter nearby in time, we obtain electron temperature, T_e , and emission measure, EM , maps for the region. These are shown in **b** and **c** respectively. All three panels are displayed on logarithmic scales, with the values for the temperature and emission measure shown in greyscale bars below **b** and **c** respectively. The units for T_e and EM are MK and m^{-3} , respectively. The EM values are per pixel.

most loops. This feature (indicated by the northward pointing arrow in Fig. 4i) may be similar to the diffuse ‘cusp’-like feature seen above the loops at the northern end of the arcade in Fig. 4h (indicated by the arrow with the open head). In fact, the latter feature is also seen in Fig. 4i.

Thus the soft X-ray images seem to show two types of ‘cusp’-like features, one occurring in the preflare stage and the other occurring in the (soft X-ray) flare–postflare stages. The preflare ‘cusp’-like structures appear to consist of several distinct, narrow ‘cusped’ loops oriented in different directions. These appear to have developed from what were clearly uncusped loops seen earlier in emission in soft X-rays. They seem to reform to uncusped loops which then appear very bright. The flare–postflare ‘cusp’-like structures appear to consist of a single cusped structure which is much larger, more diffuse and lies above the brightest parts of the bright arcade. These may have formed from magnetic loop structures not clearly visible earlier in soft X-rays. Note that the cusped loop structures observed in the flares analyzed by Tsuneta et al. (1992) and Hiei et al. (1993) were observed in the flare–postflare phases.

In the postflare stage two coronal hole-like features appeared near the dynamic arcade region, Region C. One was a dark ‘channel’ coterminous with the leading edge of the arcade of loops (indicated by the eastward-pointing arrow in Fig. 4i). The other appeared to be a transient coronal hole seen to the east of the arcade of loops of Region C (indicated by the southward-pointing arrow in Fig. 4i). Both hole-like features indicate changes in the large scale magnetic field around the region of the filament eruption and flare. In particular, they clearly show the creation of open field regions near the flaring arcade. We briefly examine the transient coronal hole in Sect. 3.4 and discuss our results in Sect. 5.

3.2.2. Temperature and emission measure

We also constructed temperature and emission measure maps of the region before the flare using the filter ratio technique for the SXT (Hara et al. 1992). To make a temperature and emission measure image we need two images taken with different soft

X-ray filters occurring close in time to each other. The practical application of the technique actually requires that we interpolate images taken in one filter to the exact time of that taken with another filter. To do that requires two images taken with the same filter before and after the desired interpolated time which do not show significant variation in features. Despite these restrictions we were able to construct several temperature and emission measure images from the portions of full-disk SXT images. Prior to the appearance of the ‘distorted’ loops there was no significant change in the temperature and emission measure of Region C compared to adjacent regions. However, as soon as the ‘distorted’ loops appeared there was an increase in both the temperature and emission measure of the loops in Region C (Fig. 8). Fig. 8a shows a portion of the soft X-ray image shown in Fig. 4d. Figs. 8b and 8c show the temperature and emission measure (on a pixel-by-pixel basis), respectively, on a logarithmic scale. The values of the temperature and emission measure displayed are shown with the color bars at the bottom of these panels. The white areas in Figs. 8b and 8c denote those points for which either the pixels are over-exposed (and hence should not be used) or for which the statistics is poor, and should be ignored. Comparing the images in Figs. 8b and 8c with temperature and emission measure maps for earlier times there is an enhancement of the temperature and emission measure for pixels in the brightened arcade from ~ 2 MK to ~ 6 MK and from $\sim 10^{48} \text{ m}^{-3}$ to $\sim 5 \times 10^{49} \text{ m}^{-3}$, respectively. The lower end of each of these ranges (i.e. ~ 2 MK and $\sim 10^{48} \text{ m}^{-3}$), as well as denoting the values of pixels in the region of the brightened arcade of ‘distorted’ loops *before* the filament activation, also denote the values of pixels of surrounding areas before and during the time of the bright ‘distorted’ loops. Thus the data demonstrate that when the loops of Region C appear to become ‘distorted’ and brighten this is associated with an increase in both emission measure and temperature.

We are unable to obtain reliable temperature and emission measure maps after this time but prior to the flare due to either the absence of two images sufficiently close together in time, due to significant changes in the features, or poor statistics.

3.3. Nearby parasitic polarity emerging flux region

A small structure labeled Region D in Fig. 4b appeared to the northeast of Region A early on May 6. This soft X-ray region overlies the parasitic polarity region referred to in Sect. 2.

It is well-known that magnetic flux emerges in the form of bipolar regions (e.g., Harvey et al. 1975; Golub et al. 1977). Therefore a parasitic polarity region is likely to consist of bipolar regions emerging in a large region of predominantly one polarity. Such regions however must have a significant polarity opposite to the surrounding region to allow them to survive and become readily apparent in magnetogram data. This is confirmed here as was mentioned in Sect. 2. In soft X-ray images the parasitic polarity emerging flux region looks like a cluster of a few small bipolar loops.

Region D may have played an important role in causing the $H\alpha$ dark filament activation and flare. This region was observed

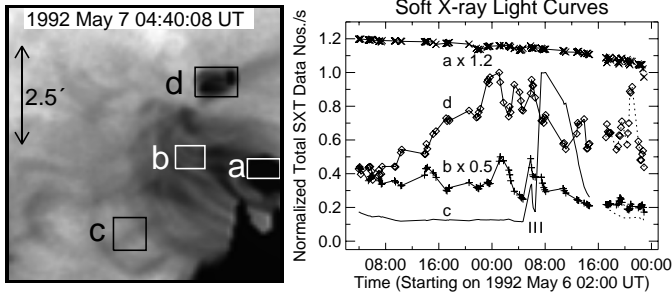


Fig. 9. The time-variation of the brightness of boxed regions in parts of aligned full-disk images taken by the *Yohkoh* SXT, including Region D. The values in each boxed region are normalized to the maximum value in each boxed region. The three tick marks below all of the light curves indicate the times of the ‘distorted’ loops, the cusped loops and the (gradual phase) flaring loops, consecutively.

to grow gradually in size and brightness until the flare on May 7. The interaction of Region D with adjacent regions may have caused the slow de-stabilization of the magnetic field configuration of Regions B and C eventually leading to the activation of the filament and the flare.

Fig. 9 shows plots of the intensity of boxed regions around parts of Regions A, B, C, and D (defined in Fig. 4b) for a series of *Yohkoh* SXT images, referred to as boxed regions a, b, c, and d, respectively. We aligned all the images to track the heliographic latitude and longitude of Region D (S07E30 at 07:23:42 UT on 1992 May 7) assuming differential rotation. The solid lines show A1.1 images taken with an exposure duration of 2668 ms, while the dotted lines show images taken with an exposure duration of 668 ms. For each boxed region we normalized the intensity curves to the maximum value for that region. Note that the intensity of the boxed region d increased with time reaching a broad peak with several episodes where the intensity rose and fell. After this the intensity of boxed region c increased suddenly (corresponding to the appearance of the brightened ‘distorted’ loops). It then dropped suddenly (corresponding to the disappearance of the bright ‘distorted’ loops and the appearance of the cusped loops). After that time (\sim 06:30 UT on 1992 May 7) it suddenly increased to a large value (corresponding to the gradual phase of the flare) and then gradually decreased in intensity. The three stages corresponding to the times of Fig. 4c, g, h (i.e., the times of the ‘distorted’, cusped, and flaring loops) are indicated by the tick marks below all of the light curves in Fig. 9. The intensity of the boxed region d appeared to drop after the appearance of the cusped loops in Region C (excluding a brief jump in intensity near 21 UT on 1992 May 7 corresponding to an isolated flaring of Region D, which in any case was after the flare in Region C). While these data do not *prove* a relation between the growth and development of boxed region d and boxed region c they are at least consistent with that suggestion.

3.4. Transient coronal hole

Following a similar procedure to that discussed in Sect. 3.3, Fig. 10 shows plots of the intensity of boxed regions around

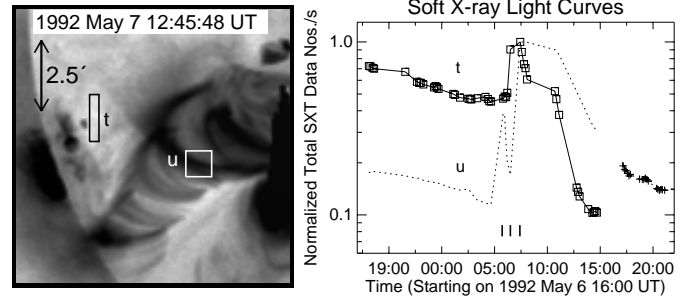


Fig. 10. The time-variation of the brightness of boxed regions in parts of aligned *Yohkoh* SXT full-disk A1.1 images, including the transient coronal hole to the east of Region C. The dotted line shows images taken with an exposure duration of 2668 ms, while the plus symbols show images taken with an exposure duration of 668 ms. The values in each boxed region are normalized to the maximum value in each boxed region. The three tick marks below all of the light curves indicate the times of the ‘distorted’ loops, the cusped loops and the (gradual phase) flaring loops, consecutively.

the transient coronal hole and the flaring arcade for a series of *Yohkoh* SXT images. In this case we aligned all the images to track the heliographic latitude and longitude of the transient coronal hole (S16E62 at 14:43:08 UT on 1992 May 7) assuming differential rotation. The solid and dotted lines show images taken with an exposure duration of 2668 ms, while the plus symbols show images taken with an exposure duration of 668 ms (for boxed region u only). The results presented here show that the transient coronal hole, indicated by about an order of magnitude decrease intensity in boxed region t, appeared \sim 6 hr after the start of the filament eruption and flare. However we have to bear in mind that since boxed region t, representing part of the eventual transient coronal hole, was near the limb it is possible that the transient coronal hole may have appeared earlier than indicated by the plots, but was not apparent because of emission from obscuring foreground field lines.

4. Comparison with Meudon $H\alpha$ observations

From an examination of the *Yohkoh* SXT images we determined the time ranges of interesting stages in the development of soft X-ray features. Comparing the SXT images and $H\alpha$ images from Paris-Meudon Observatory we carefully selected $H\alpha$ images closest in time to the times of each of these stages in the soft X-ray development. The $H\alpha$ images were obtained photographically and then digitized. The location of the solar limb for these images was determined by eye to \sim 2 arcsec. Knowing the direction for solar north for the $H\alpha$ images, and the location of the solar limb, we scaled the Meudon $H\alpha$ images down to the size of the corrected *Yohkoh* SXT images (which consisted of pixels of \sim 4.9 arcsec). The *Yohkoh* SXT images were corrected using the pointing information from the *Yohkoh* satellite attitude sensor (which is, in principle, accurate to \sim 1 arcsec). We confirmed that there was a good match between features seen in the $H\alpha$ and soft X-ray images. We estimate the accuracy of the alignment of the *Yohkoh* SXT and Meudon $H\alpha$ images shown

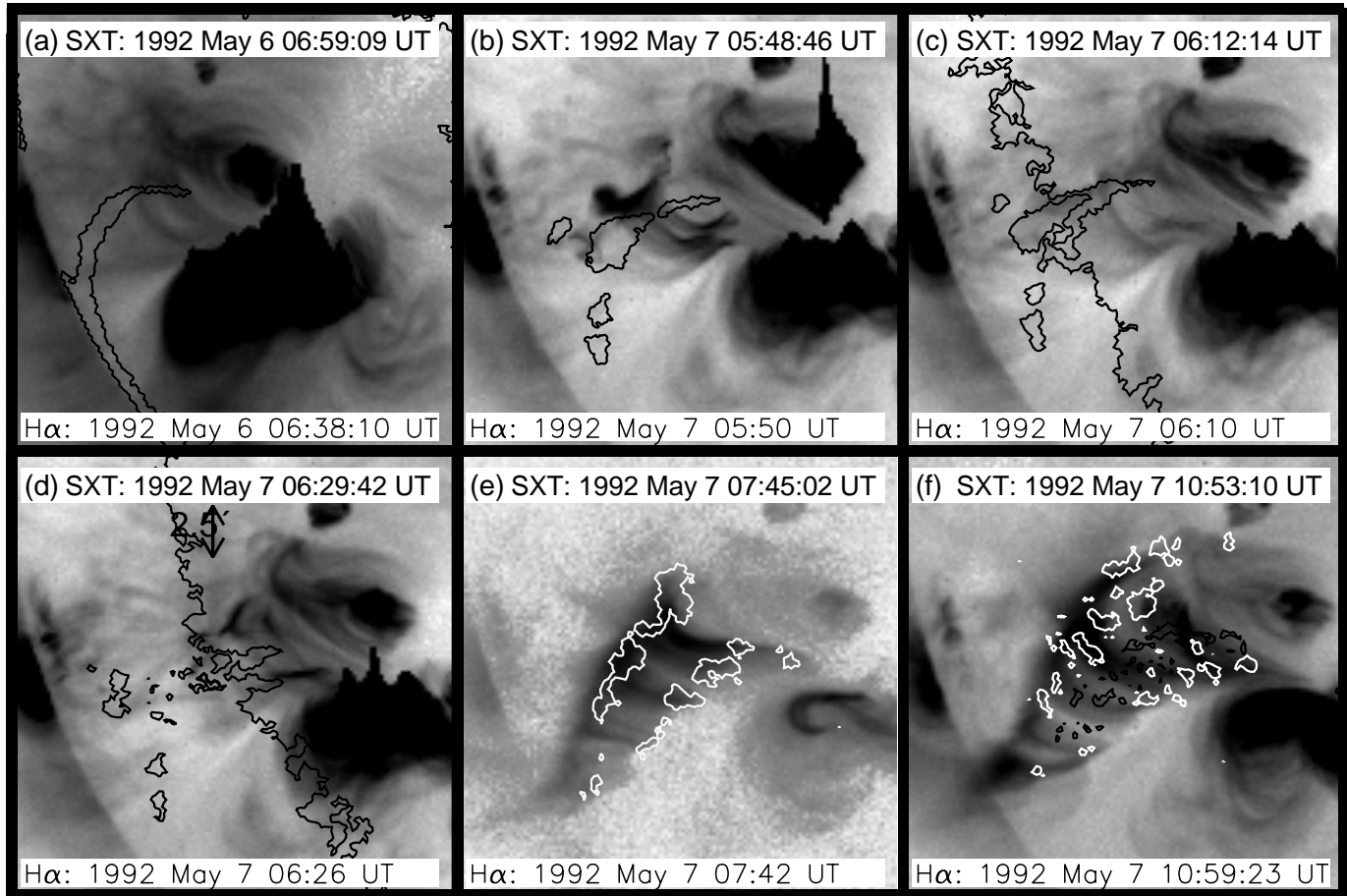


Fig. 11a–f. Portions of full-disk images taken by the *Yohkoh* SXT with selected contours of aligned $H\alpha$ images from Paris-Meudon Observatory shown overlaid. The $H\alpha$ images used are the same as those shown in Fig. 1a–f.

here to be ~ 1 SXT half resolution pixel, corresponding to ~ 4.9 arcsec. The $H\alpha$ images are shown in Fig. 1a–f. In Fig. 11a–f we show the *Yohkoh* SXT images corresponding to these $H\alpha$ images. Selected contours of the corresponding aligned $H\alpha$ images are also shown overlaid in Fig. 11a–f.

Fig. 11a shows the soft X-ray configuration during the long-lasting pre-activation stage. The contours of the aligned $H\alpha$ image nearest in time to the SXT image indicate that the $H\alpha$ dark filament appears to be located under the arcade of soft X-ray loops.

An SXT image at the time of the appearance of the ‘distorted’ loops is shown Fig. 11b. This image is part of that shown in Fig. 4d. The overlaid contours of the $H\alpha$ image show that the $H\alpha$ dark filament has begun to break up into segments, which is a common occurrence during filament activations (Martin 1980). This panel appears to show the elevation of the $H\alpha$ dark filament under the brightened ‘distorted’ soft X-ray loops.

The time of the soft X-ray ‘rail’ coincides with the time when the $H\alpha$ dark filament is elevated. Fig. 11c shows the corresponding SXT and $H\alpha$ image data. (Although we have attempted to remove limb darkening from the $H\alpha$ images, some limb darkening remains as can be seen in Fig. 1c, and by the contours

in Fig. 11c). This panel shows that the soft X-ray and $H\alpha$ ‘filaments’ overlap considerably along the line-of-sight direction.

Fig. 11d shows an SXT image at the time of the cusped loops just prior to the flare. Selected contours of the nearest $H\alpha$ image taken shortly before are also shown overlaid. The sudden disappearance of the ‘distorted’ loops and ‘rail’ seen in soft X-rays, the disappearance and eruption of the $H\alpha$ dark filament, together with the appearance of cusped soft X-ray loops lead us to conclude that both the $H\alpha$ and soft X-ray filaments are ejected at nearly the same time. If this is indeed the case then the *Yohkoh* SXT data for this event ‘show’ the ‘eruption’ of a filament on the solar disk *seen in soft X-rays*.

During the flare, the soft X-ray arcade appeared patchy in brightness with only selected loops in the arcade emitting brightly in soft X-rays. Comparing the $H\alpha$ emission shown in contours in Fig. 11e and the soft X-ray emission nearby in time, we see that the bright patches in $H\alpha$ correspond well with the footpoints of the brightest loops of the flaring arcade.

Fig. 11f shows an SXT image during the decay phase of the soft X-ray flare. The white contours show the location of $H\alpha$ emission near the ‘footpoints’ of the soft X-ray arcade of loops. The black contours show the location of the $H\alpha$ dark filament which has begun to appear below the arcade of soft X-ray loops.

5. Discussion

We now outline the main points in the development of the soft X-ray features (and by inference in the magnetic field) for this event as seen with the *Yohkoh* SXT as well as our interpretation of these observations. We describe the development with reference to various stages in the event.

5.1. Prior to $H\alpha$ filament activation

Prior to the $H\alpha$ filament activation the soft X-ray images show what appears to be a bright filamentary structure similar in size and approximate location to a dark He I 1083 nm filamentary structure (and by implication an $H\alpha$ dark filament) for overlapping times. How should the filamentary soft X-ray structure be interpreted? While *Skylab* data showed that there were elongated soft X-ray structures associated with $H\alpha$ dark filament disappearances, these structures were arcades of loops where the loops lay across the (photospheric) magnetic polarity inversion line and the filament. Note also that these X-ray structures occurred after the filament eruption, not before. Since both the ‘bright filament’ seen in soft X-rays and the (dark) filament are observed at approximately the same line-of-sight location (apparently lying low along the axis of the arcade of loops) for overlapping time intervals, this suggests a close relation between these features. However, since these ‘filaments’ have measured (electron) temperatures which are orders of magnitude different, this suggests that the plasmas of which these filaments are comprised occupy different (large-scale or small-scale) locations at a given time. This is also indicated by the imperfect overlap of the soft X-ray and He I 1083 nm filaments as seen in Fig. 6. Note that the apparently low-lying ‘bright filament’ is relatively long-lived, existing some 10–20 hr before the $H\alpha$ filament becomes activated. Possible explanations for the observations include (i) the cooler $H\alpha$ dark filament material is surrounded (at least partially) by a distinct hotter envelope which emits soft X-rays, (ii) part of the $H\alpha$ dark filament material (e.g., the inner core or outer edge) is heated to soft X-ray emitting temperatures, or (iii) there are two distinct parts to the filament, one hot and one cool, at different heights, e.g., the soft X-ray ‘filament’ may lie above (or below) the $H\alpha$ dark filamentary material.

5.2. $H\alpha$ filament activation

Although there is a gap in the *Yohkoh* SXT data and we do not see the development of the soft X-ray features from the long-lasting configuration (as shown in Fig. 4b) to the time of the ‘distorted’ loops (as shown in Figs. 4c–f) it is reasonable to suppose that the ‘bright filament’ rises and is visible in soft X-rays as the bright, straight, ‘rail’-like structure seen just under the top of the loops of the arcade of Region C. This suggestion relating the ‘rail’ to the ‘bright filament’ readily explains the disappearance of the apparently low-lying ‘bright filament’, and the sudden appearance of the ‘rail’-like feature near the top of the arcade of loops. Based on the SXT images alone, the elevation or activation of the filament occurred on 1992 May 7 sometime

between the time of the last image showing the long-lasting pre-event structures (\sim 04:46:32 UT) to the time of the first image showing the ‘distorted’ loops (\sim 05:43:16 UT). At the start of observations at Paris-Meudon Observatory on May 7 at \sim 05:50 UT the $H\alpha$ dark filament appeared elevated compared to the previous day. Moreover the ‘rail’-like soft X-ray structure overlaps considerably, along the line-of-sight direction, with the elevated $H\alpha$ dark filament as can be seen in Fig. 11c

We mentioned in Sect. 3.2.1 that the first few images showing the ‘distorted’ loops of Region C give the impression that the loops are ‘pulled’ or ‘pushed’ upwards by the ‘bright’ filament. Thus there appears to be an increase in height of the overlying arcade of loops associated with, and possibly due to, the elevation of the $H\alpha$ filament. We also found that the activation of the $H\alpha$ filament was accompanied by an increase in temperature and emission measure of the overlying loops.

The bright filamentary or linear structures seen in soft X-rays might be due to the locus of a series of brightened points at the tops of loops of an arcade caused by magnetic reconnection. For the case of the elevated ‘rail’-like structure which is seen near the top of the loops of an arcade, this suggestion, at first, appears more plausible. While it is difficult to be sure of the three-dimensional geometry of soft X-ray structures since the coronal plasma is optically thin in soft X-rays, the ‘rail’ does not appear to be above the loops, but rather under them. The order of events is also wrong for this suggestion since we might expect to see the cusped loops prior to the appearance of the locus of brightened reconnection points, opposite to the order observed. We conclude that the bright soft X-ray filaments (the low lying filament and the elevated ‘rail’) are not due to the locus the tops of loops which reconnected but are related to axial magnetic structures, perhaps part of the $H\alpha$ dark filament itself.

Kano (1994) observed linear soft X-ray features associated with $H\alpha$ filament eruptions which he termed ‘strings’. He tried to explain these soft X-ray features as the locus of reconnection points above the underlying soft X-ray arcade formed after the reconnection such as might be expected in the model proposed by Hirayama (1974), or as the heating of the core of the $H\alpha$ filament which rises but is kept below the overlying loops of the arcade which brighten in soft X-rays. For the first of these suggestions it is not obvious that enough plasma could exist at the reconnection site early in the flare to produce the observed structures or why these features are also not observed at the time of the bright flaring arcades even though magnetic reconnection is still presumed to be occurring. Moreover Kano (1994) concluded that the soft X-ray ‘strings’ seemed to lie below the loops of the arcades, not above them. The second of his suggestions has the problem that the filament cannot escape, inconsistent with the observations of the eruption of the $H\alpha$ filament.

While we cannot exclude entirely that the ‘distorted’ loops, ‘rail’-like structure, and some of the flux loops may simply be due to line-of-sight effects caused by the orientation of soft X-ray features, including the tops of loop, the $H\alpha$ data generally support our suggested interpretation of the soft X-ray data. We point out that if it was not for the last frame in our data just before the flare, it would not have been possible to state so clearly that

the filament ‘erupted’ based on soft X-ray images alone. This leads us to advise caution interpreting similar data.

What is the magnetic structure supporting the bright soft X-ray and $H\alpha$ dark filaments? One possibility is that the $H\alpha$ filament might be contained within one or more twisted magnetic flux ropes which suspend the filamentary material but isolate it from the hotter surrounding plasma. If this were the case, then eruption of the $H\alpha$ filament would be the same as the eruption of the magnetic flux ropes. The suggestion that the filament lies within a twisted magnetic flux tube was suggested earlier by Rust (1976) and Rust & Kumar (1994). These models consider the filament and arcade as part of a large single structure. However, the observations reported in this paper strongly suggest that the filament is a separate structure from the overlying arcade of loops and is able to *interact* with it.

Roy & Tang (1975) showed that the activation of an $H\alpha$ filament was associated with an increase in unresolved soft X-ray emission while Rust et al. (1975) showed that there was an enhancement of spatially resolved soft X-ray emission in the general vicinity of a filament activation. Roy & Tang (1975) suggested that the soft X-ray emission associated with a filament activation is due to the compression of overlying fields by the expanding filament. Similar suggestions were also made by Webb et al. (1976). For the event described in this paper we observed an increase in soft X-ray emission from overlying loops in association with the elevation of the $H\alpha$ filament ~ 45 min before the filament eruption. We are not sure whether compression of the overlying loops alone can account for the soft X-ray emission observed. It is certainly not obvious that there is sufficient plasma in the corona which could emit and continue to emit soft X-rays. Also it is not merely the tops of the loops that are bright in soft X-rays but most of the coronal loops, including the inferred footpoints of the loops. Compression of the overlying loops would cause a high pressure region to exist at the tops of the loops of the arcade which might be expected to drive ablation of chromospheric plasma into the loop. To determine whether compression of the overlying loops is a feasible mechanism to explain the preflare soft X-ray emission, detailed modeling would be required. An alternative possibility we would like to suggest is that the initial enhancement of soft X-ray emission of the overlying loops is caused by an interaction of the magnetic field of the elevated filament with the magnetic field of the overlying loops leading to the energization of particles and heating of chromospheric plasma which fills the loops.

Although we do not have information on the photospheric velocity field, nor have we seen photospheric vector magnetograms for this event, we find no clear evidence for energy storage or build-up by shearing motions of the coronal field near the footpoints from soft X-ray images of coronal loops as seen in images taken with the SXT. This null observation is mentioned because some authors (e.g., Zuccarello et al. 1987; Longbottom & Priest 1994) have suggested that energy may be built up by photospheric (or sub-photospheric) motions of already emerged loops and that this energy may be released suddenly activating the filament and causing the flare. The X-

ray observations reported here do not support the hypothesis that the loops are highly sheared due to horizontal motions at the photosphere. We also do not find any evidence for a highly sheared inner arcade, as suggested in the model of Moore & Roumeliotis (1992). These authors argued in favor of a model where there is a low-lying highly sheared field region along the magnetic polarity inversion line underneath a less-sheared closed magnetic field region. While *Yohkoh* SXT images may show soft X-ray structures for active region arcades which could be interpreted in this way, the suggested geometry is not consistent with the observations of quiet region arcades, including the one examined in this paper. We did find localized brightenings near the northern footpoint of the clear loop seen arching over the ‘rail’. However this does not seem to be related to motion of the footpoints of the loops of the arcade. This and the apparently ‘distorted’ loops may instead be related to the interaction of the overlying magnetic field lines with the field lines of the activated $H\alpha$ filament. We conclude that the magnetic energy released in the flare discussed in this paper is probably not associated with shearing motions of magnetic field lines at the photosphere. Note that while the idea that magnetic shear is caused by shearing motions of the footpoints of already emerged loops is widely used in some filament eruption and flare models, especially numerical models, Wang (1994) argues that there is little observational support for this suggestion. Instead he argues that magnetic shear develops from the interaction of different magnetic flux regions.

As mentioned in Sect. 3.3 a parasitic polarity region, which emerged near the Region C arcade from which the filament eventually erupted, appeared to grow in size and soft X-ray brightness. This emerging flux region may have slowly de-stabilized the magnetic field configuration of the region from which the filament erupted. Although, as mentioned above, the geometry proposed for the flaring arcade in the model of Moore & Roumeliotis (1992) does not agree with the observations of the flare examined here, these authors also emphasized the possible role of a slow destabilizing mechanism in ejective flares, including the situation with emerging flux away from the magnetic polarity inversion line but under the large-scale bipolar magnetic field of the arcade region. Schmieder et al. (1996) suggested that surges, filament eruptions and flares occur in the vicinity of parasitic polarity regions. Furthermore, Feynman & Martin (1995) showed in both statistical and case studies that those coronal mass ejections associated with the eruption of filaments are strongly associated with the emergence of new magnetic flux in the vicinity of the filament prior to eruption. The observations reported in this paper are consistent with these suggestions and findings.

5.3. $H\alpha$ filament disappearance

Immediately prior to the flare, the configuration in Region C changed to a number of apparently cusped loops with no ‘rail’ visible. Based on the SXT images alone, the ‘eruption’ of the ‘rail’ seemed to occur between the last image showing ‘distorted’ loops without cusps at $\sim 06:20:40$ UT on 1992

May 7 and the first image showing (faintly) the cusped loops at $\sim 06:27:24$ UT on 1992 May 7. The $H\alpha$ data from Paris-Meudon Observatory indicate that the main body of the $H\alpha$ dark filament began to fade and break up $\sim 06:21$ – $06:24$ UT on May 7. At $\sim 06:26$ UT on May 7 it was almost completely faded and the next image taken at $\sim 06:30$ UT on May 7 showed that the $H\alpha$ dark filament had disappeared.

It has been reported that in some filament activations the filament has different parts which behave differently. For example, Tang (1986) showed evidence for a filament eruption which seemed to consist of two parts, the upper part being ejected and the lower part remaining. Some of the observations reported here could be interpreted as the filament having consisted of two parts, an $H\alpha$ dark filament and an overlying soft X-ray filament. Note, however, that for this event *both* the $H\alpha$ and soft X-ray filaments appear to have been ejected. Despite this, the $H\alpha$ filament does reform later but appears to be different in structure (Mouradian et al. 1998). While the soft X-ray ‘filament’ may have no direct connection with the $H\alpha$ filamentary material, e.g., if there is a separate soft X-ray emitting ‘filament’ above the $H\alpha$ filament or if the $H\alpha$ filament is surrounded by an envelope which emits soft X-rays, it is also possible that the soft X-ray emitting structure might be due to material which was part of the $H\alpha$ filament at an earlier stage heated to soft X-ray emitting temperatures. We note that the elevated soft X-ray filament appears brighter and more clearly visible than the apparently low-lying soft X-ray filament. Moreover there is reasonably good overlap of the elevated soft X-ray filament and the $H\alpha$ filament. While the $H\alpha$ observations for the event described in this paper show that the filament disappeared because it was ejected, rather than heated, some heating of the $H\alpha$ filament is likely to have occurred.

5.4. Flare

The subsequent configuration of the region seen in soft X-ray images was during the decay phase of the flare and showed a bright arcade of loops in Region C. This observation seems to suggest that the cusped loops seen earlier had reformed to uncusped loops.

As discussed in Sect. 3.2.1, the ‘tail’ features seen at the end of the arcade may be associated with the bright $H\alpha$ surge seen at the limb. The soft X-ray features indicate mass motions and their topology shows the magnetic field changes associated with the filament eruption and flare. It is even possible that the ‘tails’ may be due to ejection and heating associated with parts of the $H\alpha$ filament. $H\alpha$ observations from Paris-Meudon Observatory show that the filament segments f5 and f6 shown labeled in Figs. 1b–d began to disappear at $\sim 06:36$ UT and $\sim 06:50$ UT, respectively. These filament segments might be related to the soft X-ray tail indicated by the eastward pointing arrow with the solid head in Fig. 4h. This suggestion is consistent with our general interpretation associating a bright soft X-ray filament with the activation and eruption of an $H\alpha$ dark filament. At the time of the ‘tails’ we see a diffuse cusp at the north end of the arcade. After the ‘tails’ disappear we also see a diffuse cusp nearby.

Magnetic reconnection of magnetic field lines above the bright arcade is one possible explanation for the diffuse cusped loops. The observations therefore suggest that magnetic reconnection might have proceeded northwest to southeast along the arcade, or occurred in the northwest first and later in the southeast.

The association of the eruption of an $H\alpha$ filament and an enhancement of soft X-ray emission has been well-established (e.g., Webb et al. 1976). These authors and others have shown that the eruption of an $H\alpha$ filament is followed by a bright soft X-ray emitting arcade region.

A number of authors (e.g., Sturrock 1966; Hirayama 1974; Kopp & Pneuman 1976) proposed a model to describe the eruption of a dark filament and flare including the creation of an arcade visible in soft X-rays. In such models a rising filament pulls the overlying magnetic field (loops) outward into a highly elongated shape. Oppositely directed magnetic field lines (of the overlying loops) below the filament are assumed to be pushed together and then reconnect releasing the stored magnetic energy and forming an arcade below the filament which is bright in soft X-rays. In the development of the event described in this paper we do not observe the sort of elongation of the magnetic field envisaged in these models. This conclusion should be qualified with the fact that the last image we see before the image with the cusped loops was taken ~ 7 min earlier. It is conceivable that there was a sudden elongation of the loops between these two images or at the time of the last image. The stretching of the overlying loops would then be expected to lead to a reduction of the particle number density inside the loops and hence reduced soft X-ray emission. However the similarity of loop heights for clearly discerned loops in images at the time of the cusped loops and before the cusped loops would then have to be explained. One possible explanation is that the middle section of the filament erupts causing that region to appear dim, while the ends of the filament are in the process of erupting and show cusps. Another explanation for the apparently cusped loops seen in the SXT images is that they are due either to line-of-sight effects of loops that are actually being stretched out but which are not in fact cusped loops, or due to heating of parts of the $H\alpha$ filament to soft X-ray emitting temperatures. We cannot exclude these possibilities.

We emphasize that we also see no evidence for inward flows of soft X-ray structures to a reconnection site below the soft X-ray linear feature (or ‘rail’), despite the fact that magnetic features in the vicinity are ‘visible’ in soft X-rays. Cusped loops are formed but these seem to be at nearly the same height as the uncusped (but ‘distorted’) loops seen immediately before. This is apparent if we look at the clearly distinguishable loop seen arching over the ‘rail’ feature indicated by the southward-pointing arrow in Fig. 4f. This loop can be identified (by the most northerly arrow) in Fig. 4g. Thus the filament, which was just below the tops of the ‘distorted’ loops appeared to break through the arcade by cutting the loops at their tops.

5.5. Transient coronal hole

During the postflare phase the large arcade of bright loops expanded in size and decreased in soft X-ray intensity. As was mentioned earlier a transient coronal hole formed to the east of the flaring arcade and a dark coronal channel appeared adjacent to the west edge of the arcade. The appearance of short-lived coronal holes in association with filament eruptions and flares has been reported previously (e.g., Solodina et al. 1977; Harvey & Sheeley 1979; Rust 1983). These indicate that the magnetic field on a large spatial scale is altered. In particular, they unambiguously demonstrate the creation of open field structures by the filament eruption and flare process. The transient coronal hole feature for this event was pointed out earlier by Kozuka et al. (1995). These authors suggested that the Type II radio bursts associated with the flare was later seen as an interplanetary shock (inferred from the scintillation of radio waves from a quasar). They concluded that the shock started with a nearly constant speed stage and was followed by a decelerating stage. Kozuka et al. (1995) suggested that the nearly constant speed shock was driven by a high-speed stream emanating from the transient coronal hole. Note, however, for this event the transient coronal hole was not apparent immediately at the time of the start of the flare, but ~ 6 hr afterwards. Thus the shock associated with the flare probably started within several minutes of the impulsive phase (which is the typical time interval which metric Type II bursts follow Type III bursts [one signature of flare primary energy release] as seen in solar radio spectroheliograms). This is long before the time the transient coronal was seen. Watanabe et al. (1992) argued that the formation of the transient coronal hole in this event destabilized the filament resulting in the filament eruption and flare. However, the data for this event indicate that the filament eruption occurred long before the appearance of the transient coronal hole. It is possible that the transient coronal hole did occur earlier but was not seen because its location near to the east limb means that emission from overlying field lines could have ‘masked’ its appearance. The significance of the creation of these open magnetic field line regions and whether they have any association with meter wave Type II bursts or interplanetary shock associated with flares still remain open questions. Transient coronal holes do appear to be closely associated with filament eruptions, soft X-ray arcades of loops and flares. However the nature of the association is not fully understood at the moment.

5.6. Possible scenario

The soft X-ray images for this event together with $H\alpha$ data seem to indicate the following possible scenario for the sequence of events. The $H\alpha$ dark filament initially lies low under the arcade of loops. Later a soft X-ray filament is seen, which may be due to heating of part of the $H\alpha$ filament or from a separate magnetic structure. Due to the destabilization of the magnetic field of the arcade by a parasitic polarity emerging flux region the $H\alpha$ dark filament (and the soft X-ray filament) rise and push against, but remain contained below, the overlying loops. The interaction of

the magnetic field of the rising flux tube with the overlying magnetic field causes the overlying loops to become ‘distorted’ and bright in soft X-rays. Part of the $H\alpha$ dark filament is probably heated and this is visible as a bright linear soft X-ray feature just below the loops of the arcade. Eventually continued interaction of the magnetic field of the overlying loops with the magnetic field of the filament causes the magnetic field of the loops to open. At least parts of both the soft X-ray and $H\alpha$ filamentary material are ejected and cusped loops are formed. The cusped loops are observed in soft X-rays because they were brightened earlier. Heating of the chromosphere causes the $H\alpha$ emission at the footpoints and the ablation of chromospheric material into the loops filling them with hot dense plasma. This causes an increase in temperature and emission measure of the soft X-ray loops. The cusped loops reform to uncusped loops. Tracers of the magnetic field changes are shown by the ‘tail’ features and ‘knot’ visible at the southern end of the bright arcade. These show the end of the ejection of the filamentary material and the changes in the magnetic field of the arcade. If magnetic reconnection occurred, then it appears to have occurred first in the north end of the arcade and then in the south end of the arcade. The changes in the magnetic field extend beyond the immediate vicinity of the flaring arcade to include the creation of open magnetic field regions nearby.

6. Conclusions

In this paper we have presented observations and analysis which reveal new features and details in the evolutionary sequence of the filament activation and eruption process.

The observations presented here show a soft X-ray filament apparently lying low under a large arcade of loops some 10–20 hr before the $H\alpha$ filament becomes activated. The apparently low-lying soft X-ray filament is found to be co-existent and partially co-spatial along the line-of-sight with a dark He I 1083 nm filamentary structure which we take as a proxy for the $H\alpha$ dark filament. The soft X-ray images also show the disappearance of the apparently low-lying soft X-ray filament and the appearance of a bright linear feature under a brightened arcade of ‘distorted’ loops. This linear feature appears at the same time the $H\alpha$ filament becomes activated. The elevated linear soft X-ray structure is co-spatial, along the line-of-sight direction, with the elevated $H\alpha$ dark filament. Both the apparently low-lying and elevated linear soft X-ray structures might be part of the filament heated to soft X-ray emitting temperatures and densities or a distinct structure such as an envelope, a core, or a separate filament. We interpret the bright elevated linear soft X-ray feature as the elevation of the apparently low-lying soft X-ray filament. The overlying loops showed an increase in temperature and emission measure at the start of the activation of the $H\alpha$ filament. Shortly before the soft X-ray flare (indicated by a steep rise in the *GOES* flux) we observe apparently cusped-shaped soft X-ray loops without the elevated soft X-ray feature. These observations can be interpreted as the activation and eruption of the filament seen in soft X-rays. Moreover they show that, rather than viewing the filament and overlying arcade as part of a sin-

gle structure, they should be considered to be semi-independent structures that can interact with each other. This is an important observation that theoretical models should incorporate in future.

We also find two types of cusped loops in this event: (i) several narrow ‘cusped’ loops just prior to the flare and (ii) a single diffuse cusped structure which lies above the brightest parts of the bright arcade after the flare. These features may be due to magnetic reconnection of field lines before, as well as during and after the flare, respectively.

The observations also indicate that a nearby parasitic polarity emerging flux region may have played a role in destabilizing the arcade region resulting in the filament activation, eruption and flare.

We also observe apparent outward motion of soft X-ray emitting features at the end of the arcade which may be the soft X-ray counterpart of the reported $H\alpha$ surge on the limb. These soft X-ray features indicate mass motions of plasma associated with the eruption process. This mass may have originated from the filament itself.

The soft X-ray images clearly show that the magnetic field beyond the immediate vicinity of the arcade is significantly modified. Open-field regions, specifically a transient coronal hole and a dark coronal channel near the arcade are created. These appear to have formed some ~ 6 hr after the start of the filament eruption and flare, but may have occurred earlier.

From an examination of the morphology and temporal relations of structures in the development of the filament eruption we conclude that the nature of the magnetic reconfiguration appears to differ from that proposed in the model by Hirayama (1974) and related models. We also do not observe a highly sheared arcade underlying a less-sheared arcade as proposed in the model by Moore & Roumeliotis (1992). However we agree with their suggestion that the emergence of magnetic flux away from the magnetic polarity inversion line could slowly destabilize the large-scale magnetic field containing the filament. The brightening of the overlying loops before the disappearance of the filament is consistent with the suggestion of an interaction of the magnetic field of the filament and the overlying magnetic structures. We suggest this interaction eventually causes the field *above* the filament to reconnect creating clearly cusped loops. The opening of the overlying field lines allows the filamentary material to be ejected. The cusped loops reform to uncusped loops resulting in a flaring arcade.

Acknowledgements. J.I.K. received support from the Japan Society for the Promotion of Science (JSPS), the Royal Society, and the UK Particle Physics and Astronomy Research Council (PPARC). A.H.M. received support from JSPS, the US National Science Foundation and the National Research Council. The *Yohkoh* mission is a joint Japan-US-UK project managed by the Institute of Space & Astronautical Science (ISAS) of Japan. The *Yohkoh* Soft X-ray Telescope experiment is a joint Japan-US collaboration involving the National Astronomical Observatory of Japan (NAOJ), the University of Tokyo, and the Lockheed-Martin Advanced Technology Center. *Yohkoh* is supported by ISAS, NASA, and PPARC. *GOES* data are courtesy of the World Data Center A for Solar-Terrestrial Physics, NGDC, NOAA, 325 Broadway, Boulder CO 80303, USA. The magnetogram and He I

1083 nm spectroheliogram data are courtesy of the NSO, Kitt Peak, USA.

References

- Feynman J., Martin S. F., 1995, JGR 100(A3), 3355
 Golub L., Krieger A. S., Harvey J. W., Vaiana G. S., 1977, Solar Phys. 53, 111
 Hanaoka Y., Kurokawa K., Enome S., et al., 1994, PASJ 46, 205
 Hara H., Tsuneta S., Lemen J. R., Acton L. W., McTiernan J. M., 1992, PASJ 44, L135
 Harvey J. W., Sheeley N. R., Jr., 1979, Space Sci. Rev. 23, 139
 Harvey K. L., Harvey J. W., Martin S. F., 1975, Solar Phys. 40, 87
 Hiei E., Hundhausen A. J., Sime D. G., 1993, GRL 20(24), 2785
 Hirayama T., 1974, Solar Phys. 34, 323
 Howard R. F., Harvey J. W., Forgach S., 1990, Solar Phys. 130, 295
 Hudson H. S., Acton L. W., Sterling A. C., et al., 1994, Non-thermal Effects in Slow Flares. In: Y. Uchida, T. Watanabe, K. Shibata, H. S. Hudson (eds.), X-ray Solar Physics from *Yohkoh*, Universal Academy Press, Tokyo, p. 143
 Kahler S., 1977, ApJ 214, 891
 Kano R., 1994, The Time Evolution of X-ray Structures during Filament Eruptions. In: Y. Uchida, T. Watanabe, K. Shibata, H. S. Hudson (eds.), X-ray Solar Physics from *Yohkoh*, Universal Academy Press, Tokyo, p. 273
 Khan J. I., Uchida Y., McAllister A. H., Watanabe T., 1994, *Yohkoh* Soft X-ray Observations Related to a Prominence Eruption and Arcade Flare on 7 May 1992, In: Y. Uchida, T. Watanabe, K. Shibata, H. S. Hudson (eds.), X-ray Solar Physics from *Yohkoh*, Universal Academy Press, Tokyo, p. 201
 Kopp R. A., Pneuman G. W., 1976, Solar Phys. 50, 85
 Kosugi T., Makishima K., Murakami T., et al., 1991, Solar Phys. 136, 17
 Kozuka Y., Watanabe T., Kojima M., et al., 1995, PASJ 47, 377
 Longbottom A. W., Hood A. W., 1994, Solar Phys. 155, 267
 Martin S. F., 1980, Solar Phys. 68, 217
 Martes M.-J., Michard R., Soru-Iscovici I., 1966, Annales d’Astrophysique 29, 245
 McAllister A. H., Dryer M., McIntosh P., Singer H., 1996a, JGR 101(A6), 13497
 McAllister A. H., Kurokawa H., Shibata K., Nitta N., 1996b, Solar Phys. 169, 123
 Moore R. L., Roumeliotis G., 1992, Triggering of eruptive flares: Destabilization of the preflare magnetic field configuration, In: Z. Švestka, B. V. Jackson, M. E. Machado (eds.), IAU Colloq. 133, Eruptive Solar Flares, Springer-Verlag, Berlin, p. 69
 Mouradian Z., Soru-Escout I., Pojoga S., 1995, Solar Phys. 158, 269
 Mouradian Z., Soru-Escout I., Hiei E., et al., 1998, Solar Phys. in press
 Nelson G. J., Melrose D. B., 1985, Type II bursts, In: D. J. McLean, N. R. Labrum (eds.), Solar Radiophysics: Studies of Emission from the Sun at Metre Wavelengths, Cambridge University Press, Cambridge, p. 333
 Ogawara Y., Takano T., Kato T., et al., 1991, Solar Phys. 136, 1
 Pallavicini R., Serio S., Vaiana G. S., 1977, ApJ 216, 108
 Priest E. R., 1989, Dynamics and Structure of Quiescent Solar Prominences, Kluwer Academic Publishers, Dordrecht
 Roy J.-R., Tang F., 1975, Solar Phys. 42, 425
 Rust D. M., 1976, Solar Phys. 47, 21
 Rust D. M., 1983, Space Sci. Rev. 34, 21
 Rust D. M., Kumar A., 1994, Solar Phys. 155, 69
 Rust D. M., Nakagawa Y., Neupert W. M., 1975, Solar Phys. 41, 397

- Schmieder B., Rovira M., Simnett G. M., Fontenla J. M., Tandberg-Hanssen, E., 1996, *A&A* 308, 957
- Sheeley N. R., Jr., Bohlin J. D., Brueckner G. E., et al., 1975, *Solar Phys.* 45, 377
- Sheeley N. R., Jr., Howard R. A., Koomen M. J., Michels D. J., 1983, *ApJ* 272, 349
- Smith S. F., Ramsey H. E., 1967, *Solar Phys.* 2, 158
- Solodyna C. V., Krieger A. S., Nolte J. T., 1977, *Solar Phys.* 54, 123
- Sturrock P. A., 1966, *Nat* 211, 695
- Tandberg-Hanssen E., 1995, *The Nature of Solar Prominences*, Kluwer Academic Publishers, Dordrecht
- Tang F., 1986, *Solar Phys.* 107, 233
- Tsuneta S., Acton L. W., Bruner M. E., et al., 1991, *Solar Phys.* 136, 37
- Tsuneta S., Hara H., Shimizu T., et al., 1992, *PASJ* 44, L63
- Uchida Y., 1974, *Solar Phys.* 39, 431
- Wang J., 1994, *Solar Phys.* 155, 285
- Watanabe T., Kozuka Y., Ohyama M., et al., 1992, *PASJ* 44, L199
- Webb D. F., Hundhausen A. J., 1987, *Solar Phys.* 108, 383
- Webb D. F., Krieger A. S., Rust D. M., 1976, *Solar Phys.* 48, 159
- Zuccarello F., Burm H., Kuperus M., Raadu M., Spicer D. S., 1987, *A&A* 180, 218